SnAgCu/Cu钎焊接头等温时效下组织性能分析

杨思佳[1]， 杨晓华[2]
(1. 福州大学 材料学院，福州 350002; 2. 福州大学 测试中心，福州 350002)

摘 要： Sn3.0Ag0.5Cu/Cu钎焊接头在125，150，175 ℃三种温度下分别进行了36，72，216，360，720 h等温时效，对钎焊接头微观组织及力学性能在时效过程中的演变规律进行了研究. 结果表明，界面金属间化合物(IMC)在横截面上呈细小锯齿状，随着时效温度升高及时间延长，界面IMC的尺寸不断增加，增长速度随时效温度升高而增加，随时效时间延长而减小. 界面IMC齿数不断减少、齿径变大、齿高变长、齿距变宽. 分析得出一种科学的表征界面IMC尺寸的方法. 计算时效后界面IMC层等效厚度，发现界面IMC层的等效厚度与时效时间及温度之间具有一定的数学关系，同时可计算出界面IMC的生长激活能为88 kJ/mol. 此外研究了时效对钎焊接头抗拉强度的影响，随时效时间增加接头抗拉强度先增大后减小，这主要与接头残余应力释放及界面IMC的演变有关.

关键词： 无铅焊料； 等温时效； 显微组织； 力学性能
中图分类号： TG407 **文献标识码：** A **文章编号：** 0253-360X(2013)05-0083-04

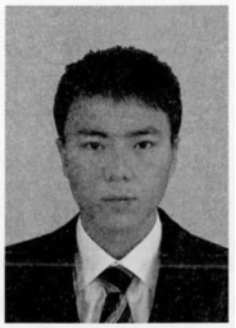

杨思佳

0 序 言

21世纪以来，科技飞速发展，人们对电子产品的追求达到了一个前所未有的高度，电子产品飞速更新换代导致每年将有巨大数量的电子垃圾产生. 由于传统的Sn/Pb钎料中含有大量的重金属元素Pb，其对人体及自然界都有严重的危害，例如2010年2月湖南250名儿童血铅含量超标，这对儿童的身心都造成了不可恢复的创伤. 随着人们环保意识逐渐增强，各国开始关注电子产品中的铅污染，并立法限制或禁止使用含铅产品，欧盟27国于2006年7月1日同时实施了WEEE/RoHS法令，该法令禁止在其成员国生产和销售含铅的电子产品，中国于2007年3月也开始了对含铅钎料使用的限制[1-3].

随着含铅钎料的限制使用，工业界和学术界已经开展了大量的无铅钎焊材料的研究. 目前而言，二元无铅钎料主要有Sn/Cu，Sn/Ag，Sn/Bi，Sn/Zn，Sn/In等体系，但其电化学性能、润湿性及力学性能等方面都和传统的Sn/Pb钎料相差很远. 在这种情况下，各国研究人员开始加大对三元及多元合金体系无铅钎料的研究. 目前研究比较深入、电子封装应用较广泛的三元合金体系主要有Sn-Ag-Cu，Sn-Zn-Al两种，而SnAgCu系钎料被认为是最有潜力替代传统Sn/Pb钎料的. SnAgCu系钎料已有几个专利成分[4]：美国NEMI推荐使用Sn3.9Ag0.6Cu合金钎料，日本JEITA则推荐使用Sn3.0Ag0.5Cu合金钎料，欧盟则推荐的是Sn3.8Ag0.7Cu合金，国内授权的专利合金是SnAgCuRE(ZL02123528.7).

文中选择Sn3.0Ag0.5Cu合金钎料为研究对象，分析不同热时效温度、时效时间对钎焊接头组织、力学性能的影响，为高性能低成本无铅钎料提供数据基础和理论指导.

1 试验方法

试验采用日本JEITA推荐的Sn3.0Ag0.5Cu合金钎料，钎焊基底为纯度99.9%(质量分数)的纯铜，将材料用夹具固定放入回流焊炉中，加热至280 ℃，取出自然冷却. 接头尺寸形状如图1，钎焊工艺曲线如图2.

将钎焊接头分别放入恒温干燥箱中进行热时效处理，时效温度分别为125，150，175 ℃，时效时间分别为36，72，216，360，720 h.

将钎焊接头制成金相试样，用金相显微镜观察金相组织并拍取照片. 借助SEM分析接头界面及断口内部组织. 利用JeDa金相分析系统Version2.0分析金相形貌，在截面宽度一定的情况下，计算各截

收稿日期： 2012-04-18
基金项目： 国家自然科学基金资助项目(50871004)

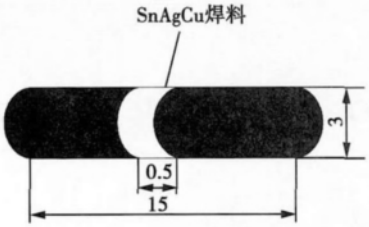

图 1 SnAgCu/Cu 钎焊接头尺寸(mm)

Fig. 1 Sketch map of SnAgCu/Cu solder joint

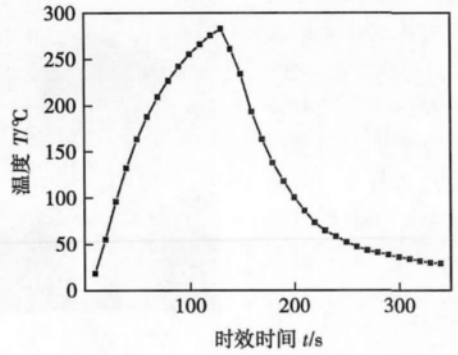

图 2 SnAgCu/Cu 钎焊温度曲线

Fig. 2 Welding temperature curve of SnAgCu/Cu solder joint

面的界面 IMC 面积 S,得出 IMC 层的等效厚度. 利用 INSTRON5948 微拉伸机测试钎焊接头的力学性能,拉伸速度为 0.6 mm/min,作用力为 100 N(非最大作用力).

2 试验结果与分析

2.1 IMC 尺度的表征方法

图 3a 所示为利用 13% 的硝酸酒精腐蚀后的接头界面 IMC 层 SEM 顶视图,钎焊界面焊料方向长出了许多细小的 IMC 齿. 图 3b 是图 3a 的垂直截面,图 3b 中白色部分是用软件染色的界面 IMC,还可看出界面 IMC 是在一个薄的 IMC 平层上长出了许多细小 IMC 齿,其形状极其不规则,因此无法直接测量其准确的厚度. 利用 JeDa 金相分析系统 Version2.0 分析其金相形貌,可以计算出每个时效条件下一组精确的二维截面面积 S,再除以截面的宽度 d,则可计算出 IMC 层的等效厚度 $x=S/d$.

2.2 界面组织形态的变化

用金相显微镜对时效前、后的接头组织进行了观察. 图 4 是接头在 150 ℃下时效不同时间的横截面金相形貌. 钎焊接头由 3 个区域组成,即铜基体、IMC 层和钎料基体. 图 4a 为焊态接头的界面组织形貌,此时在界面 IMC 层的横截面上已有细小的齿

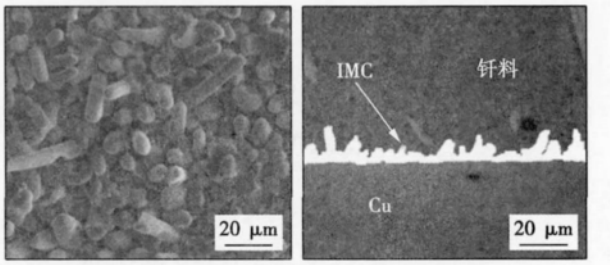

(a) 界面IMC的顶视图 (b) 界面IMC染色图

图 3 接头界面 IMC 的顶视图及染色图

Fig. 3 Top view of IMC and IMC dyeing picture

凸起出现,但 IMC 齿数较多、齿距窄、齿高小; 界面 IMC 整体尺寸较小. 在高温时效过程中,由于钎料与基体之间元素的相互扩散,界面 IMC 层会不断长大. 时效 36 ~ 216 h,IMC 齿不断向钎料内部生长,齿径变大、齿高变长、齿尖变平,如图 4b,c,d. 同时整个 IMC 平层也不断变厚,由于某些 IMC 齿的优先生长,将会出现一些 IMC 齿针被 IMC 平层吞没,时

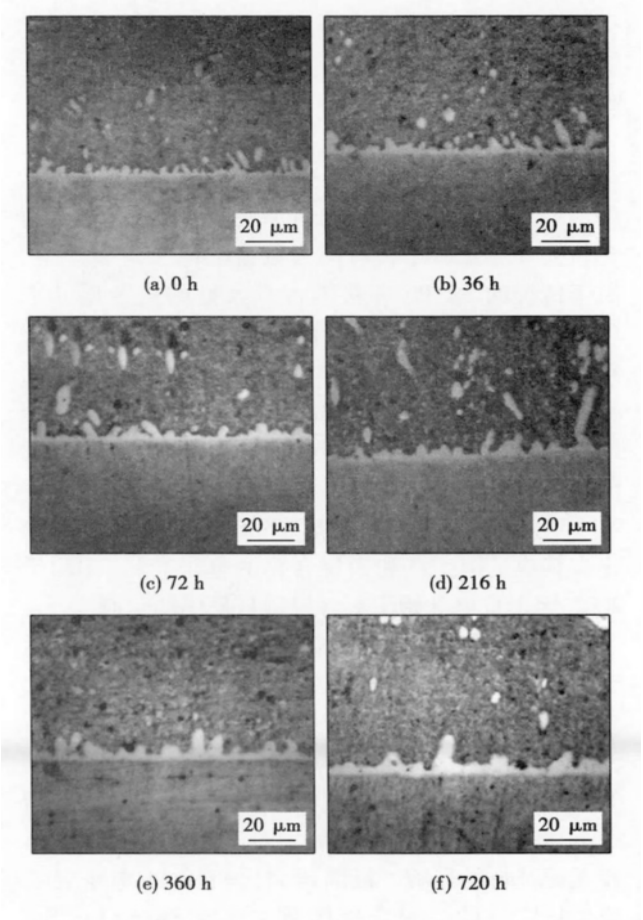

图 4 150 ℃时效不同时间界面 IMC 金相形貌

Fig. 4 Metallographic of interfacial IMC after aging at 150 ℃ for different time

效 360 h 及 720 h 后，IMC 齿数减少，平层变厚，IMC 的等效厚度也逐渐变大，如图 4e，f. 图 5 为 150 ℃，72 h 时效后界面 IMC 的扫描电镜俯视图，可以看到此时已经有部分的 IMC 齿优先生成.

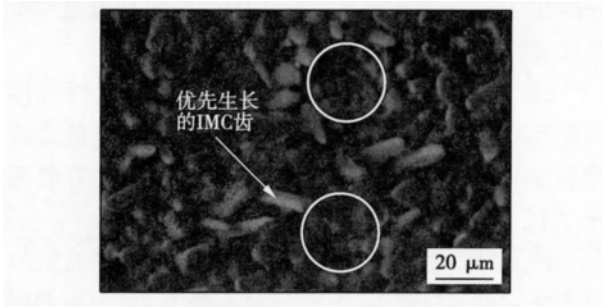

图 5　150 ℃时效 72 h 的 IMC 俯视图

Fig. 5　Vertical view of IMC after aging at 150 ℃ for 72 h

2.3　界面 IMC 的生长

时效过程中 IMC 不断生长，界面层不断变厚. 一般认为，钎焊接头在服役过程中，钎焊接头界面 IMC 的生长主要由扩散机制决定. 幂率方程被广泛用于描述固态阶段 IMC 的生长，即 IMC 厚度随温度和时间的演变具有如下规律，即

$$x = x_0 + At^n \tag{1}$$

式中：x 为 t 时刻 IMC 的厚度；x_0 为 IMC 原始的厚度；A 为扩散系数；n 为生长指数. 由 Arrhenius 方程，A 可表示为

$$A = A_0 \exp(-\Delta H/RT) \tag{2}$$

式中：A_0 是扩散常数（ms^{-n}）；ΔH 是激活能（J/mol）；R 是 Boltzmann 常数（8.314 J/(mol·K)）；T 是绝对温度（K），结合以上两式，得

$$x - x_0 = A_0 \exp(-\Delta H/RT)\, t^n \tag{3}$$

利用文中所述计算 IMC 等效厚度的方法，对 3 种温度下、6 个不同时效时间的界面 IMC 尺寸进行了计算. 图 6 为界面 IMC 等效厚度与时效时间 1/2 次方之间的关系曲线，随着时效时间的延长 IMC 的生长速度减慢，这是由于已经生成的 IMC 层对元素的扩散会起着阻碍作用；125 ℃下的生长速度明显低于 150 ℃和 175 ℃，这是由于温度越高，扩散越活跃，扩散系数越大. 图 6 还可看出，利用文中所述 IMC 等效厚度计算方法所得出的 IMC 厚度与拟合的直线非常吻合，比文献[5]中图 11 更加符合 IMC 真实生长规律.

利用图 6 拟合直线斜率，结合式（1）可知 3 种温度下扩散系数分别为 $A_1 = 0.123\ 5\ \mu m/h^{1/2}$，$A_2 = 0.134\ 3\ \mu m/h^{1/2}$，$A_3 = 0.196\ 1\ \mu m/h^{1/2}$. 将 A_1，A_2，A_3 分别代入式（2）进行拟合，得到扩散系数与时效温度的关系曲线如图 7 所示. 由此可求出 IMC 生长所需的激活能为 88 kJ/mol，这个数值与 Zheng 等人[6]计算的 89.7 kJ/mol 和 Lee 等人[7]计算的 92.6 kJ/mol 十分接近.

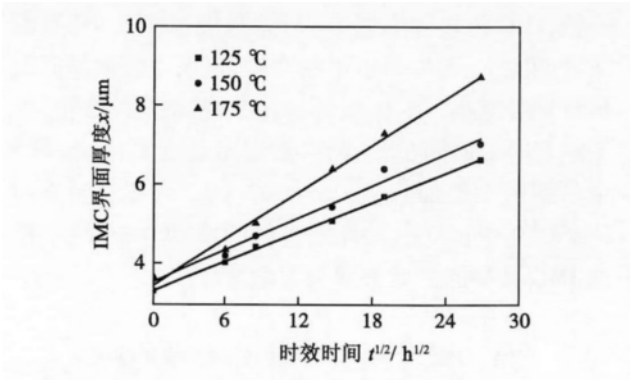

图 6　IMC 等效厚度与时效时间的关系

Fig. 6　Relationship between IMC equivalent thickness and square root of aging time

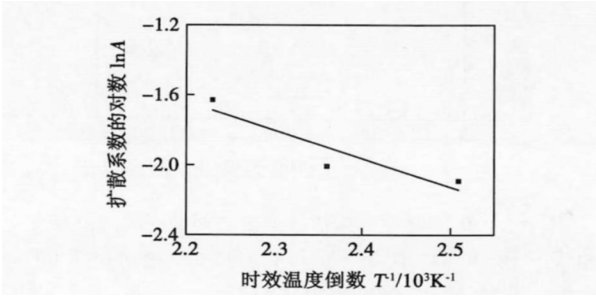

图 7　扩散系数与时效温度的关系

Fig. 7　Relationship between diffusion constant and aging time

3　时效对钎焊接头力学性能的影响

界面 IMC 属于硬脆相，塑性差. 表 1 为接头 150 ℃时效下钎料的显微硬度，采用 HXD-1000 型维氏硬度试验机，加载载荷为 0.98 N，压头为正方形，随时效时间增加钎料显微硬度下降. 图 8 为 150 ℃时效时间与接头抗拉强度的关系. 时效过程中，接头抗拉强度并不是一开始就下降，而是先有所增大，然后再下降. 平整其原因可能是钎料与母材具有不同的热导率和热膨胀系数，在升降温过程中，导致钎焊接头内部有残余应力. 短时间的时效可能会消除这种残余应力使钎焊接头抗拉强度有所提高. 但是随着时效时间延长，IMC 齿径变大、齿高变长，并且其与界面是成一定角度生长的，这就导致拉伸过程中会有一个横向剪切力；又因为 IMC 层逐渐变

平整，IMC 齿数逐渐减小，与焊料接触面减小，界面结合能减小，而焊料也不断变软，从而导致钎焊接头抗拉强度变小. 图 9 是钎焊接头断口微观形貌，可见随着时效时间延长，断口韧窝不断变大，这与图 5 中白圈内平整部分是相对应的，IMC 齿被拉断就留下了图 9 中韧窝内光滑平整的断面，而细小较平整的 IMC 被拉断后就表现为大韧窝.

表 1 150 ℃时效不同时间钎料的显微硬度

Table 1 Hardness of solder after aging at 150 ℃ for different time

时效时间 t/h	钎料硬度 H_{HV}/MPa
0	12.8
72	12.4
360	11.1
720	10.8

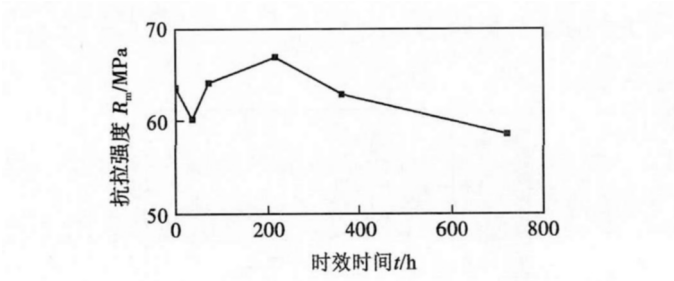

图 8 150 ℃时效接头抗拉强度与时效时间的关系

Fig. 8 Relationship between tensile-strength and aging time after aging at 150 ℃

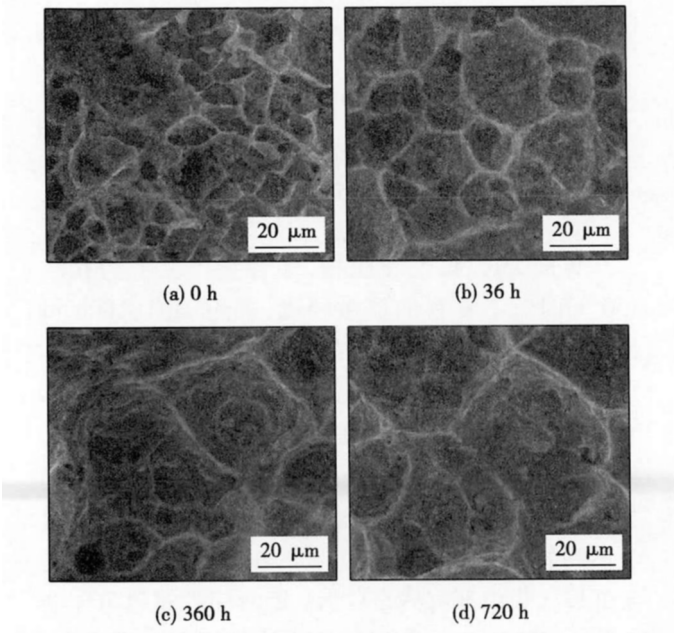

图 9 150 ℃时效不同时间钎焊接头断口形貌

Fig. 9 Tensile fracture by SEM of joints after aging at 150 ℃

4 结 论

(1) 找到一种表征 SnAgCu/Cu 钎焊界面不规则形状 IMC 厚度的科学方法，利用 JeDa 金相分析软件计算 IMC 截面面积，求出 IMC 的等效厚度. 所得等效厚度更符合 IMC 生长规律.

(2) 随时效温度升高及时效时间延长，钎焊接头界面 IMC 的等效厚度不断增加，增长速度呈放缓趋势；IMC 的等效厚度与时效时间的 1/2 次方成正比，IMC 的生长激活能为 88 kJ/mol.

(3) 钎焊接头抗拉强度随时效时间先稍有增加后不断减小，钎焊接头断口韧窝不断变大，大块 IMC 平齐断裂.

参考文献:

[1] Tong Xin. Diffusion of lead-free soldering in electronics industry in China [J]. China Population, Resources and Environment, 2007, 17(6): 66-71.

[2] 董文兴，史耀武，夏志东，等. SnAgCu 无铅钎料焊点结晶裂纹 [J]. 焊接学报，2008，29(12)：61-64.
Dong Wenxing, Shi Yaowu, Xia Zhidong, *et al*. Solidification crack of SnAgCu lead-free solder joint [J]. Transactions of the China Welding Institution, 2008, 29(12): 61-64.

[3] 罗家栋，薛松柏，曾 广，等. SnCuN ix Pr 焊接接头组织和性能分析 [J]. 焊接学报，2011，32(5)：57-60.
Luo Jiadong, Xue Songbai, Zeng Guang, *et al*. Microstructures and solderability of SnCuN ix Pr lead-free solder [J]. Transactions of the China Welding Institution, 2011, 32(5): 57-60.

[4] 史耀武，夏志东，雷永平，等. 电子组装生产的无铅技术与发展趋势 [J]. 电子工艺技术，2005，26(1)：6-9.
Shi Yaowu, Xia Zhidong, Lei Yongping, *et al*. Electronic assembly production of lead-free technology and the development tendency [J]. Electronics Process Technology, 2005, 26(1): 6-9.

[5] Li Xiaoyan, Li Fenghui, Guo Fu, *et al*. Effect of isothermal aging and thermal cycling on interfacial IMC growth and fracture behavior of SnAgCu/Cu joints [J]. Journal of Electronic Materials, 2011, 40(1): 51-61.

[6] Zheng Y, Hillman, Mchluskey P. Intermetallic growth on PWBs soldered with Sn3.8Ag0.7Cu [C] // 2002 Electronic Components Technology Conference. San Diego, CA: Institute of Electrical and Electronics Engineers Inc, 2002: 1226-1231.

[7] Lee T Y, Choi W J, Tu K N, *et al*. Morphology, kinetics and thermodynamics of solid state aging of eutectic SnPb and Pb-free solders(SnAg, SnAgCu, and SnCu) on Cu [J]. Journal of Materials Research, 2002(17): 291-301.

作者简介： 杨思佳，男，1989 年出生，硕士研究生. 主要从事 SnAgCu 无铅钎料稳定性的研究. 发表论文 1 篇. Email: ysj19890111@163.com

通讯作者： 杨晓华，女，教授. Email: xhyang@fzu.edu.cn

results showed that compared with MIG welding, low power laser-MIG hybrid welding could control the deposition process more accurately and more steadily, and could obtain more uniform microstructures.

Key words: rapid prototyping; vertical deposition; laser-arc hybrid heat source; aluminum alloy

Numerical simulation of free metal transfer of low current CO_2 arc welding based on Surface Evolver SONG Jiaqiang, XIAO Jun, ZHANG Guangjun, WU Lin (State Key Laboratory of Advanced Welding and Joining, Harbin Institute of Technology, Harbin 150001, China). pp 75-78, 98

Abstract: The force and critical sizes of metal droplet should be investigated in order to realize controlling in the free metal transfer in the CO_2 arc welding. Therefore, under the precondition of repulse force, gravity and surface tention, the numerical simulation model of free droplet of the CO_2 arc welding based on Surface Evolver is established. The free metal transfer is analyzed according to the principle of the minimum energy of a system. In addition, the effect of repulse force on the metal transfer is investigated and the connection between welding current and critical sizes of the droplet is acquired preliminarily. The investigation lays the basis for controlling the free metal transfer under low current in the next step.

Key words: CO_2 arc welding; numerical simulation; Surface Evolver; free metal transfer; repulse force

Heating characteristics of conductive polymer matrix composites and resistance welding of polymer GUO Qing[1], LI Ruiqi[1], CHEN Zheng[1], YE Guangyu[2], GAO Fei[2] (1. College of Material Science and Chemical Engineering, Harbin Engineering University, Harbin 150001, China; 2. State Key Laboratory of Advanced Welding and Joining, Harbin Institute of Technology, Harbin 150001, China). pp 79-82

Abstract: Conductive polymer matrix composites were prepared by using acrylonitrile-butadiene-styrene (ABS), conductive polyaniline (PANI) and conductive carbon black (CB). The relationship of the temperature during the welding with the welding time under different welding voltage was examined. The resistance welding of polycarbonate (PC) was investigated by using the conductive polymer matrix composites as a heating resistor. Results indicate that the welding voltage and welding time have a strong effect on the interface bonding in resistance welding. Within a suitable power, the optimal welding temperature can be obtained in fixed time. A desired joint is formed at the welding interface due to the mutual melting phenomenon between polymer resistor and base materials, and the joint strength reaches up to 25.4 MPa. A novel method for plastic resistance welding using conductive composite materials as the heating device was explored in this research work.

Key words: resistance welding; plastic welding; conductive polyaniline; conductive composite

Microstructure and mechanical properties of SnAgCu/Cu solder joint during isothermal aging YANG Sijia[1], YANG Xiaohua[2] (1. School of Materials Science and Engineering, Fuzhou University, Fuzhou 350002, China; 2. Instrumentation Analysis and Measurement Center, Fuzhou University, Fuzhou 350002, China). pp 83-86

Abstract: The Sn3.0Ag0.5Cu/Cu lead-free solder and Cu joints were isothermally aged at 125, 150 and 175 ℃ for 36, 72, 216, 360 and 720 h. The microstructure and mechanical properties of the solder joints were studied. The results showed, after soldering the interfacial intermetallic compounds (IMC) of solder joints were small serrate. The size of interfacial IMC was found to increase with the aging temperature and aging time. The IMC growth rate increased with aging temperature but decreased with aging time. With the increase of aging time, the amount of IMC serration decreased, and its diameter, height and width became bigger, higher and wider respectively. Through analysis of the interfacial IMC, a scientific method to characterify IMC size was found. When the IMC equivalent thickness was calculated, the quantitative relationship between IMC equivalent thickness and aging time/temperature was established. The IMC activation energy is 88 kJ/mol. In addition, the relationship between isothermal aging and tensile strength was developed. The tensile strength firstly increased and then decreased with the aging time, which could be attributed to the welding residual stress relaxation and the IMC evolution.

Key words: lead-free solder; isothermal aging; microstructure; mechanical performance

Finite element anlysis of temperature field in multi-pass welding of thick steel plate XU Guoxiang[1], DU Baoshuai[2], DONG Zaisheng[3], ZHU Jing[1] (1. Key Laboratory for Advanced Welding Technology of Jiangsu Province, Jiangsu Univeristy of Science and Technology, Zhenjiang 212003, China; 2. Shandong Electric Power Research Institute, Jinan 250002, China; 3. Jinan Iron & Steel Group Corporation, Jinan 250101, China). pp 87-90

Abstract: Considering the effect of groove on distribution of welding heat input and geormetric feature of weld cross section, the heat source model for multi-pass welding of thick ultrafine grained Q460 high strengh steel plate was developed. The shapes and sizes of weld bead and HAZ were simulated by using ANSYS software, which agreed well with the experimental data. The thermal cycles in multi-pass welding of ultrafine grained steel were computed and quantitatively analyzed. The results show that subsequent weld passes have an important influence on peak temperature, retention time of high temperature and cooling time of thermal cycle in HAZ along the whole thickness direction of workpiece, and thus the heat input for subsequent weld passes or temperature difference among two adjacent weld passes should be controlled strictly.

Key words: thick steel plate; multipass welding; temperature field; numerical simulation

Simulation of nugget formation process in multi-points projection welding and its application WANG Rui[1], AO Sansan[2], LUO Zhen[2], ZHI Derui[1], WEI Fushui[3] (1. School of Science, Tianjin University of Commerce, Tianjin 300134, China; 2. School of Materials Science and Engineering, Tianjin University, Tianjin 300072, China; 3. School of Automation, Tianjin University of Technology, Tianjin 300384, China). pp 91-94